AN

CEAC-TR-2000-0107

MULTIAXIAL YIELDING BEHAVIOR AND ELASTOPLASTIC COLLAPSE MODELING OF THERMOPLASTIC LINERS

S. S. Wang[1], T. P. Yu[1], A. Selvarathinam[1] and J. F. Mason[2]

[1]Composites Engineering and Applications Center (CEAC), University of Houston, Houston, TX.
[2]ATOFINA Chemicals, Inc., King of Prussia, PA.

NOVEMBER 2000

COMPOSITES ENGINEERING AND APPLICATIONS CENTER
FOR PETROLEUM EXPLORATION AND PRODUCTION

UNIVERSITY OF HOUSTON
HOUSTON, TX 77204-0900

CEAC-TR-00-0104

MULTIAXIAL YIELDING BEHAVIOR AND ELASTOPLASTIC COLLAPSE MODELING OF THERMOPLASTIC LINERS

by

S. S. Wang[1], T. P. Yu[1], A. Selvarathinam[1] and J. F. Mason[2]

Composites Engineering and Applications Center, and Department of Mechanical Engineering University of Houston 4800 Calhoun Road Houston, TX 77204-0903

November, 2000

[1] Composites Engineering and Applications Center (CEAC), University of Houston, Houston, TX.
[2] ATOFINA Chemicals, Inc., King of Prussia, PA.

ABSTRACT

A combined experimental, theoretical and computational study has been conducted to investigate elastoplastic buckling and postbuckling collapse of thermoplastic liners, especially plasticized thermoplastic polyamide polymers, in composite pipes. Multiaxial plastic yielding experiments have been performed first on a plasticized polyamide BESNO-P40 liner material to determine its yield criteria and flow constitutive equations at different stress biaxiality ratios and temperatures. A combined theoretical and computational modeling effort has also been conducted to determine plastic buckling modes, critical annular pressure loading and postbuckling collapse behavior of thermoplastic liners with various geometric, loading and defect parameters. Based on the experimental and computational results obtained and the analytical methods and models developed, many important conclusions have been drawn in the study for future design, analysis, testing and safe applications of thermoplastic liners used in a composite pipe.

TABLE OF CONTENTS

1. INTRODUCTION

A liner is the component of a composite tube that forms the inner barrier surface in contact with the fluid being transported by the tube. The liner is normally continuous and joint-free. The liner may be inserted into a prefabricated tube or pipe, or it may serve as a mandrel around which fibers and the matrix of a composite structure are wound. As such, the liner must have properties that make it resistant to chemical attack by the matrix. The liner must also have mechanical and thermal properties that permit sufficient strength and rigidity to prevent damage, and serve as a reliable mandrel during the winding process and through the normally high-temperature process of composite matrix curing. Secondly, during normal use of the fiber/matrix composite tube, the liner serves as the pressure barrier that prevents leakage of the tube contents into the composite body, and also prevents chemical attack on the composite by the contents of the tube. Because one of the most attractive justifications for using composites in off-shore operations is light-weight, the liner must be of low specific gravity or thin, preferably both, while maintaining the required mechanical and chemical properties.

Rilsan* polyamide-11 (PA-11) has been used for 30 years by all major manufacturers of non-bonded flexible pipes as a pressure barrier, the anti-wear layers between steel layers, and as an external sheathing [1]. Since 1995 it has been used as a liner for carbon steel pipes transporting crude oil and gas [2, 3], and produced water from wellheads to processing facilities. The Rilsan liner has been shown to have excellent aging behavior in service [4-6]. More recently the excellent resistance to damage by explosive decompression was reported [7]. These applications specify the use of a flexible, plasticized grade of the material, designated as BESNO-P40-TL.

The more rigid unplasticized grade of Rilsan polyamide-11, BESVO-TL, is an excellent candidate as a liner for composite tubing and pipe applications. Previously we reported the mechanical, physical and chemical resistance properties of BESVO-TL, and early results of our work on modeling the collapse behavior of the material [8]. Since then the computational modeling work has progressed to cover nonlinear liner collapse simulations that include both elastic and plastic deformation phases [9].

In this paper we present the completed experiments and analysis of multiaxial yielding behavior of the BESNO-P40-TL grade of Rilsan polyamide-11 at a variety of temperatures and stress biaxiality ratios. This information has enabled the subsequent development of a full elastoplastic collapse model that accurately predicts the critical liner buckling pressures and postbuckling collapse processes as a function of many variables including: temperature, thickness, installed stress state and manufacturing defects. The analytical and computational methods for elastoplastic liner buckling and postbuckling collapse simulation, as well as the results derived from the analysis are reported in this paper.

---

* Rilsan is an internationally registered trademark of ATOFINA Chemicals, Inc. Rilsan is manufactured and sold by ATOFINA Chemicals, Inc., Philadelphia, PA, and Paris, France.

2. MULTIAXIAL PLASTIC YIELDING EXPERIMENTS

2.1 Materials and Specimen Design

The plasticized thermoplastic-polymer liner investigated in the present study, BESNO-P40, was manufactured by an extrusion process and supplied in a tubular form. The average outer diameter and wall thickness of the tube were measured as 1.484" and 0.087", respectively. The length of the specimens tested was all 14" with a gauge length of 10" since 2" of the specimen length was assimilated within the grips at each end.

2.2 Test System and Experimental Setup

The experimental setup consisted of a 5 gpm, 10 HP hydraulic pump that drove a pressure intensifier by applying a pressure up to 3,000 psi. A closed-loop servohydraulic-controlled pressure intensifier with a pressure amplification factor of 8, pressurized the resident fluid (in this case water) to a maximum of 24 ksi. The pressurized water was then applied internal to the specimen resulting in a multi-axial stress state in hoop and axial directions. In addition to the axial stress arising from internal pressurization an external axial stress state was superimposed on the specimen, employing by an ATS constant-displacement test machine.

The grips employed in the experiment were specially designed to facilitate the application of both the axial load and internal pressure to the specimens. A specially designed temperature-controlled oven was built in-house to heat the specimen.

Several transducers were employed to collect data during the experiments. A load cell measured the load applied to the specimen while a pressure transducer was used to measure the internal pressure of the specimen. Two strain gauges mounted in the hoop direction were used to measure the hoop strains. In addition, axial and hoop extensometers were also employed to measure axial and hoop strains, respectively. A 100 Mhz, 486 PC with a 16-bit Strawberry Tree data acquisition card and a data acquisition software written in-house were employed to collect data during the experiments.

2.3 Experimental Procedure

Specimen dimensions were initially measured and then the specimen was mounted in the grips and loaded onto the ATS test machine. If the test had to be run at an elevated temperature, the specimen was initially filled with hot water at a prescribed temperature to reach equilibrium. The oven was subsequently placed on a specially constructed stand such that it enclosed the entire gauge section of the test specimen. Sufficient time was allowed to bring the system to equilibrium before the experiment commenced.

All the experiments in the present study were performed at a constant strain rate. Noting that the stress-state in the tubular specimen is biaxial, a single parameter, namely, the equivalent strain rate, is employed to express the plastic yielding and flow deformation. The equivalent strain rate is defined as [10]

$$(\Delta\dot{\bar{\varepsilon}})^2 = \frac{4}{9}\{\frac{1}{2}[(\Delta\dot{\varepsilon}_{11} - \Delta\dot{\varepsilon}_{22})^2 + (\Delta\dot{\varepsilon}_{11} - \Delta\dot{\varepsilon}_{33})^2 + (\Delta\dot{\varepsilon}_{22} - \Delta\dot{\varepsilon}_{33})^2] + 3(\Delta\dot{\varepsilon}_{12}{}^2 + \Delta\dot{\varepsilon}_{13}{}^2 + \Delta\dot{\varepsilon}_{23}{}^2) \quad (1)$$

where, $\Delta\dot{\bar{\varepsilon}}$ an incremental equivalent plastic strain rate, and $\Delta\dot{\varepsilon}_{ij}$ (i, j=1,2,3) are components of the incremental plastic strain rate. The above equation for the present two-dimensional loading case reduces to

$$\dot{\bar{\varepsilon}} = \frac{2}{3}\sqrt{\dot{\varepsilon}_z{}^2 + \dot{\varepsilon}_\theta{}^2 - \dot{\varepsilon}_z\dot{\varepsilon}_\theta} \quad (2)$$

where z, θ and r are along axial, hoop and radial directions, respectively, and '$\bullet$' signifies differentiation with respect to time. All the tests were performed at a constant equivalent strain rate of $\dot{\bar{\varepsilon}} = 0.67*10^{-3}/\text{sec} \pm \Delta\dot{\bar{\varepsilon}}$, where $\Delta\dot{\bar{\varepsilon}}$ was typically 7% of $\dot{\bar{\varepsilon}}$. The aforementioned value for the equivalent strain rate was chosen, based on earlier experiments on unplasticized thermoplastic polyamide P-11 [8, 11].

3. ELASTOPLASTIC BUCKLING AND POSTBUCKLING COLLAPSE MODELING

3.1 Thermoplastic Liner Constitutive Equations

Based on the experimental results of the thermoplastic polymer mechanical properties (Figs. 1 and 2), the thermoplastic liner can be shown to have nonlinear material constitutive equations. In the present formulation, the total strain ε in the liner may be expressed as

$$\varepsilon = \varepsilon^{el} + \varepsilon^{pl} \tag{3}$$

where ε^{el} and ε^{pl} are elastic and plastic strain components, respectively. Elastic stress and strain components can be related by the well-known Hooke's law. The plastic strain components of the liner material constitutive equations may be derived with a yield function and the associated flow rule. The general theory requires that the thermoplastic liner material constitutive equations satisfy the uniaxial stress-plastic-strain relationship in a degenerated case. The experimentally determined elastoplastic stress-strain behavior of a plasticized polyamide BESNO-P40 thermoplastic liner material exhibits significant nonlinearity and is modeled by an elastoplastic analysis procedure. Subsequent plastic deformations are modeled by successive multilinear approximations of the nonlinear liner constitutive equations [9].

3.2 Elastoplastic Buckling and Postbuckling Analysis for Confined Liner Collapse

As shown in Figs. 3 and 4, the liner will be deformed downward at point A, while the annular pressure between the outer pipe and the liner increases. The load-displacement curve is expressed by the liner displacement δ and annular pressure p, as shown in Fig. 5. The δ increases with the annular pressure before reaching the critical state, p_c. After the critical state, the liner exhibits postbuckling deformation and subsequently collapses, where the load-displacement response shows a negative stiffness. The annular pressure must decrease to retain its equilibrium. In addition to the collapse behavior, there is concern about material and geometric nonlinearity prior to buckling, a load-deflection (Riks) analysis must be employed in the finite element method for modeling such behavior. The detail algorithm of the modified Riks method can be found in Ref.[12].

To investigate the postbuckling problem, one must treat the problem with continuous nonlinear deformation instead of discontinuous bifurcation. This can be accomplished by introducing an initial imperfection geometry so that a proper deformation in the buckling mode is account for before the critical load is reached. In this study, a fraction of the first eigenmode of a unconfined liner is used as the initial geometric imperfection. By performing a load-displacement (Riks) analysis, other important nonlinear effects, such as material inelasticity or contact can be included.

3.3 Numerical Procedure and Algorithm

Detailed numerical simulation of a thermoplastic liner collapse within an outer tubing, when subjected to an increasing annular pressure, has been conducted for different cases under investigation (Fig. 3). The simulation is performed, using the aforementioned

nonlinear finite element method, to evaluate the liner buckling modes, the collapse load and subsequent postbuckling deformation of the collapsed liner. The outer pipe is relatively rigid, and its deformation is negligible, compared with that in the liner. Normal contact without friction is assumed between the pipe surface and the deformed thermoplastic liner. Solid contact elements are introduced between the liner and the surrounding pipe to ensure that nonlinear interface contact conditions are properly account for.

4. RESULTS AND DISCUSSION

4.1 Multiaxial Plastic Deformation and Yield Criteria

4.1.1 Effects of Stress Biaxiality Ratio on Plastic Deformation

In Fig. 1, the thermoplastic liner yielding behavior and plastic flow at room temperature have been obtained for the polyamide BESNO-P40. The yield stresses of the material at different stress biaxiality ratios k are also determined (based on the ASTM 2% offset method). In all the experiments conducted at selected stress biaxiality ratios (k = 0, 0.4, 1.22 and 2), the axial flow stress increases monotonically with the axial strain. From the results it can be seen that adding a small hoop stress on the axial loading increases the yield stress while an added large hoop stress may depresses the yield stress in the thermoplastic liner material.

The aforementioned observations also hold true for the high-temperature cases studied (Fig. 2). However, at a higher temperature, due to thermally activated softening, the yield stress is significantly reduced. For example, the yield stress of 1.48 ksi at k=0 and T=20°C was reduced by thirty three percent to 0.99 ksi at T=60°C.

4.1.2 Multiaxial Yielding Criteria

In Fig. 6, yielding surfaces of the BESNO-P40 at three different temperatures namely T=20°C, 60°C and 80°C, are obtained. The anisotropic shear yielding envelopes for the BESNO-P40 at different temperature are shown by solid lines while experimental data are shown as the discrete data points. The anisotropic shear yielding envelope was determined, using the following well known relationship [13]:

$$\left(\frac{\sigma_\theta}{X}\right)^2+\left(\frac{\sigma_z}{Y}\right)^2-2H\sigma_\theta\sigma_z=1 \tag{4}$$

where

$$H=\frac{1}{Y^2}-\frac{1}{2Z^2} \tag{5}$$

In the above equations, σ_θ and σ_z are hoop and axial stresses, respectively, and X, Y and Z are yield strengths along hoop, axial and radial directions, respectively. From direct experimental observations and based on the fact that the experimental data follow the anisotropic shear yielding criteria well clearly indicate that the yielding and plastic flow in the thermoplastic liner studied here are governed by a shear yielding mechanism.

It should be noted that in the figure at least three data points were obtained for each stress state investigated at a strain rate within $0.67*10^{-3}$/sec $\pm$ $\Delta\dot{\bar{\varepsilon}}$, which were subsequently used to construct the yielding envelopes. Note that most of the experimental data points lie

very close to the shear yield surface albeit some of them were obtained at a strain rate outside this range.

For all temperatures studied it is observed that the thermoplastic liner yielding strength in hoop and axial directions differed by less than five percent. However, the radial yielding strength was consistently higher than those in other two directions by as much as thirty five percent. This anisotropic yielding may be a result of plastic-flow induced orientation in the polymer. Also noted that at a higher temperature the difference between the yield stresses at a similar stress state (k) is less significant.

4.2 Elastoplastic Buckling and Postbuckling Collapse Analysis

4.2.1 Elastoplastic Buckling Modes and Critical Loads of Liners under Annular Pressure

Numerical results of plastic buckling and postbuckling collapse of a thermoplastic liner under increasing annular pressure p are expressed by the change in the maximum separation δ (Figs. 3 and 4) between the liner and the surrounding pipe.

The relationship between the maximum liner-pipe separation δ and an increasing annular pressure p is shown in Fig. 5 for a 4-inch pipe with a neutral-fit 0.15 inch thick thermoplastic liner. The δ is found to increase with the annular pressure before reaching the critical state, p_c. At the critical pressure, the liner collapses plastically and continues to deform excessively thereafter in the postbuckling state. Comparing with the solution obtained from an elastic collapse analysis (Fig.5), the critical p_c for elastoplastic collapse of the thermoplastic liner is 12% lower.

In a neutral-fit case ($\eta = 0$), the overall liner deformations obtained from the elastoplastic collapse modeling at several loading levels are shown in Fig. 7. After the liner collapses at the critical pressure, plastic yielding in the liner continues to develop extensively. The liner starts its yielding in the top portion where the maximum bending deformation occurs. The plastic deformation continue even the load bearing decreases during the collapse process.

4.2.2 Effect of Liner Thickness on Liner Buckling and Postbuckling Collapse

The effect of liner thickness on the critical collapse pressure inside a 4-inch pipe is shown in Fig. 8. The critical liner collapse pressure is found to increase linearly with the liner thickness. During the postbuckling collapse process, the relationships between the separations δ and the annular pressure p in a pipe with three distinct liner thicknesses are given in Fig. 9. As expected, a thicker liner carries a higher collapse resistance.

4.2.3 Effect of Liner Thickness Variation on Liner Buckling and Postbuckling Collapse

A liner with wall thickness variation (Fig. 10-a) along the circumferential direction is recognized as a common manufacturing defect. The effect of the defect on its buckling and

postbuckling collapse behavior is studied and shown in Fig. 10-b. From the results, it can be seen that under an increasing annular pressure the liner starts buckling in the thinner portion first and changes its buckling mode from that of uniform thickness case. The effect of liner thickness variation on the critical collapse pressure is shown in Fig. 11. It is interesting to note that the critical liner collapse pressure increases monotonically with the liner thickness variation (t_2-t_1) - an unexpected beneficial effect.

During the postbuckling collapse process, liner separations δ under an increasing annular pressure in the pipe (D_0 = 4 inch) containing two distinct (t_2-t_1) variations are given in Fig. 12.

4.2.4 Effect of Liner Tightness on Liner Buckling and Postbuckling Collapse

An important concern in installation and operations of a thermoplastic liner is the tightness of the liner introduced into a pipe and its effect on liner collapse. As shown in Fig. 13, a liner tightness parameter η is introduced here as:

$$\eta = [R_{o\,(liner)} - R_{i\,(pipe)}] / R_{o\,(liner)} \tag{6}$$

where $R_{o\,(liner)}$ is the outer radius of the liner, and $R_{i\,(pipe)}$, the inner radius of the pipe.

The effect of liner tightness on the critical collapse pressure of the liner in a pipe is investigated and the results are shown in Fig. 14. The critical liner collapse pressure is found to increase monotonically with increasing tightness. During the liner collapse process, liner separations δ from the pipe in three distinct η cases are given in Fig. 15. As expected, the tighter the liner is, the higher the collapse resistance it exhibits. The loose liner exhibits the lowest collapse resistance among the three cases studied.

For a tightly fitted liner (η = 1.55%) in a pipe, the liner is initially under a compressive hoop strain exerted by the outer pipe. The critical collapse annular pressure leads to a liner deformation shape shown in Fig. 16-b. Since the initial tighting operation introduces a significant amount of hoop compression, the liner starts to yield plastically at several locations simultaneously.

For a loosely fitted liner case (η = -3.1%), plastic deformation in the liner resembles that in a neutral-fit case. The collapsed liner is more likely to deform to a lateral direction as shown in Fig. 17-b.

4.2.5 Effect of Temperature on Liner Buckling and Postbuckling Collapse

The effect of temperature on the critical collapse pressure is studied also for a thermoplastic liner with different tightnesses in a pipe. The results for the temperature effect are shown in Fig. 18. Since the liner is more compliant at a high temperature, the critical liner collapse pressure decreases monotonically with increasing temperature in all cases studied. From the results, at any given temperature change, it is clear that the tightest fit liner

causes the biggest reduction in its collapse resistance. The loose fit liner, as expected, is least affected by the temperature change in its pressure-bearing capability.

5. CONCLUSIONS

A combined experimental, theoretical and computational study has been conducted to investigate elastoplastic buckling and postbuckling collapse of thermoplastic liners, especially plasticized thermoplastic polyamide polymers, in composite pipes. Multiaxial plastic yielding experiments have been performed first on a plasticized polyamide BESNO-P40 liner material to determine its yield criteria and flow constitutive equations at different stress biaxiality ratios and temperatures. A combined theoretical and computational modeling effort has also been conducted to determine plastic buckling modes, critical annular pressure loading and postbuckling collapse behavior of thermoplastic liners with various geometric, loading and defect parameters. Based on the experimental results obtained and the analytical methods and models developed, the following conclusions may be drawn in the study.

(1). The applied biaxial stress state significantly affects the yield strength and subsequent plastic deformations in a thermoplastic liner at all temperatures studied.

(2). The experimental data obtained from multiaxial plastic yielding tests of the plasticized polyamide BESBO-P40 liner are found to follow well the Hill's anisotropic yield criterion at all three temperatures studied. This, together with the detailed observations made in the experiments, indicates that the thermoplastic liner yielding is a shear-dominated plastic flow deformation.

(3). The inherent plastic yielding criteria and flow constitutive equations of thermoplastic liners must be included in any thermoplastic liner buckling and collapse study. Failure to include the nonlinear polymer properties results in significant over-estimation of the critical liner collapse resistance.

(4). The critical collapse (annular) pressure of a thermoplastic liner in a composite pipe is found to increase linearly with liner wall thickness – an important and useful relationship for design and analysis of liner resistance in a pipe.

(5). The non-uniform liner wall thickness with its variation given in the study can lead to a complete change in buckling modes and subsequent plastic deformation. It has also been found that the critical collapse pressure increases with liner wall-thickness variation – an unexpected beneficial effect on liner collapse resistance.

(6). Introducing proper liner tightness in its installation substantially increases the liner collapse resistance. For example, introducing a 1.55% tight-fit liner in a 4 inch-diameter pipe may double is critical annular collapse pressure.

(7). Collapse modes of plastic buckling and postbuckling deformations in a thermoplastic liner are governed by liner tightness during installation. A neutral-fit liner exhibits totally different failure modes from that of a tight-fit liner in a composite pipe.

(8). A high-temperature environment significantly reduces the critical collapse pressure for a liner in a composite pipe. At any given temperature it has been found a tighter liner suffers a greater reduction in its collapse resistance.

6. REFERENCES

[1] F. Dawans, J. Jarrin, T. Lefevre and M. Pelisson, "Improved Thermoplastic Materials for Offshore Flexible Pipes," *Proceeding of 1986 Offshore Technology Conference*, Paper No.: OTC-5231, Houston, TX, May 1986.

[2] J. F. Mason, "Pipe Liners for Corrosive High-Temperature Oil and Gas Production Applications," *Materials Performance, 37*:9, 1998, pp 34-40.

[3] D. Lebsack and D. Hawn, "Internal Pipeline Rehabilitation Using Polyamide Liners,"*Materials Performance, 37*:3, 1998, pp 24-27.

[4] J. Mason, "Pipeline Liner Material Wears Well in Test of Field Specimens," *Oil and Gas Journal, 97*:42, 1999, pp 76-82.

[5] D. Lebsack, "Pipeline Liner Design and Operating Experience for Sour Gas Pipelines," *Pipeline & Gas Journal*, January 2000, pp 77-80.

[6] A. Berry, "Installation of Polyimide-11 Liners for Sour Service Using Loose-Fit Technology,", *Proceedings of Corrosion/2000*, Paper No.: 00781, NACE International, March 2000.

[7] J. Mason and J. D. Alkire, "Effect of Rapid Decompression Conditions on Liner Materials," *Proceedings of Corrosion/2000*, Paper No.: 00782, NACE International, March 2000.

[8] J. F. Mason, P. Dang, F. Mondini and S. S. Wang, "Thermoplastic Liners for Composite Tubes: Properties and Performance," *Composite Materials for Offshore Operations* – 2, S. S. Wang, J. G. Williams and K. H. Lo, Eds., American Bureau of Shipping, New York, 1999, pp. 537-554.

[9] S. S. Wang, J. Mason and T. Yu, "Effect of Tightness on Thermoplastic Liner Collapse Resistance," *Proceedings of Corrosion/2000*, Paper No: 00789, NACE International, March 2000.

[10] N. P. Suh and A. P. L. Turner, *Elements of Mechanical Behavior of Solids*, McGraw-Hill Book Company, New York, 1975.

[11] F. Mondini and S. S. Wang, "Multiaxial Plastic Deformation of Polyamide Polymers at Different Temperatures," *CEAC Technical Report*, University of Houston, 1998.

[12] *ABAQUS Theory Manual*, Hibbitt, Karlsson & Sorensen, Inc., Pawtucket, RI, 2000.

[13] G. E. Dieter, *Mechanical Mettalurgy*, McGraw-Hill Book Company, 1988.

7. ACKNOWLEDGEMENT

The research reported in this paper was supported in part by ATOFINA CHEMICALS, Inc. through a grant to the Composites Engineering and Applications Center (CEAC) at the University of Houston. The authors gratefully acknowledge the support for this work.

8. FIGURES

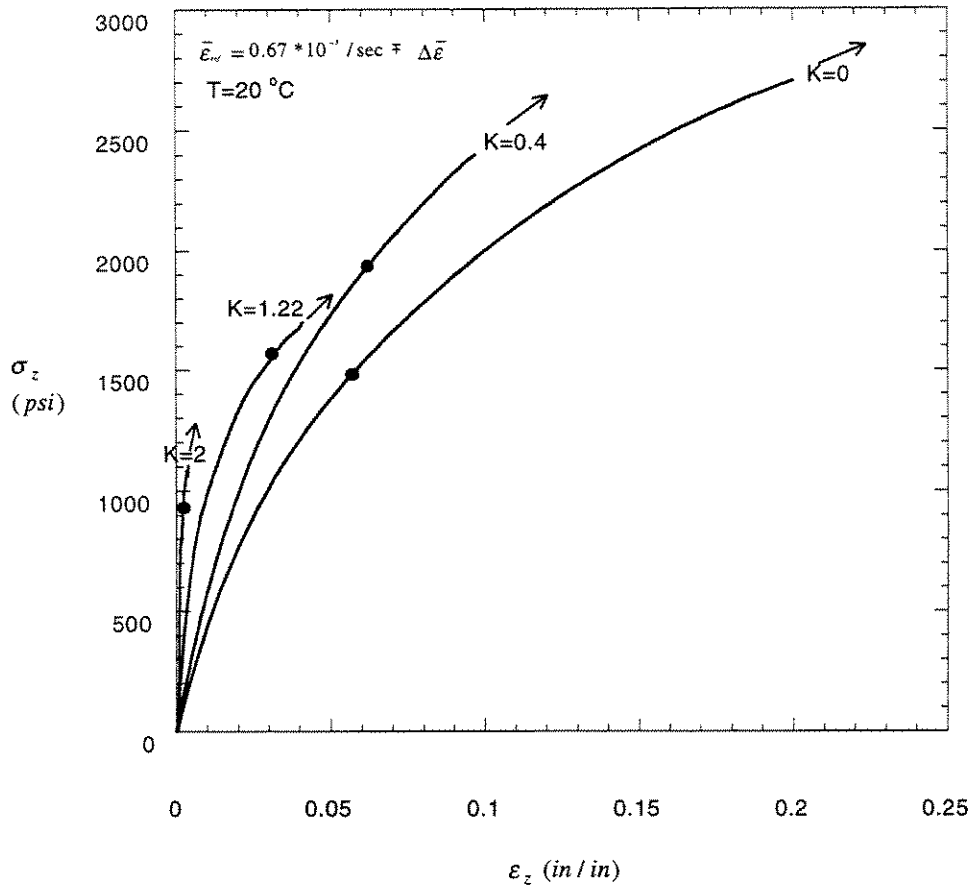

Fig. 1 – Effect of stress biaxility ratio on elastoplastic deformation of thermoplastic BESNO-P40 at T=20°C (Yield stresses are indicated by '•').

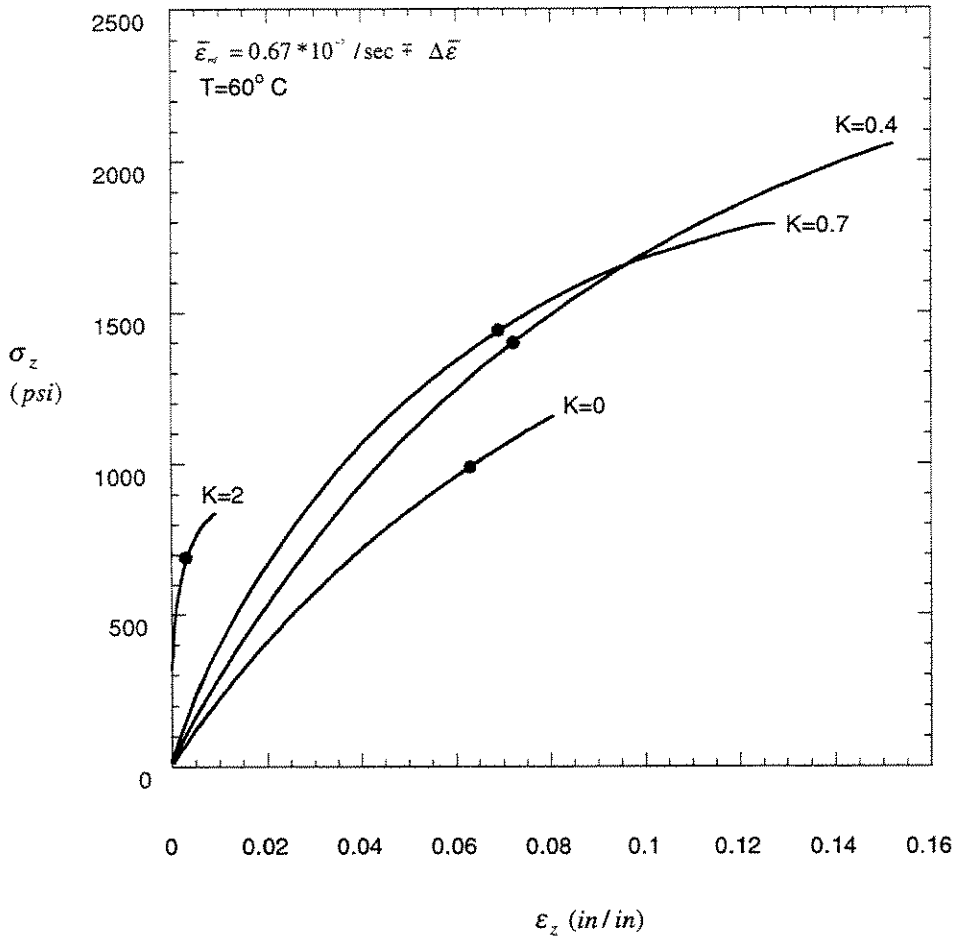

Fig. 2 - Effect of stress biaxility ratio on elastoplastic deformation of thermoplastic BESNO-P40 at T=60°C (Yield stresses are indicated by '•').

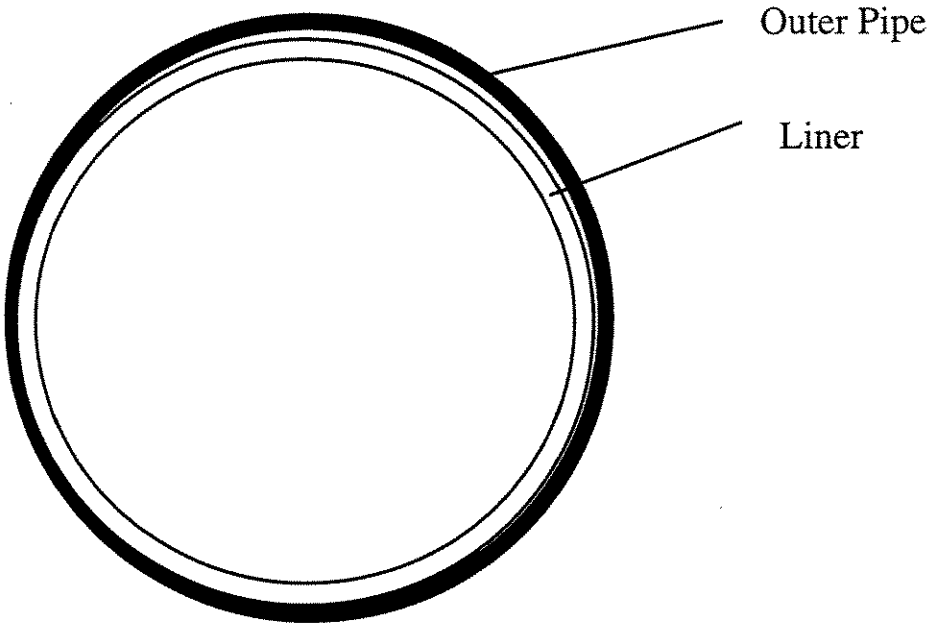

Fig. 3 - Schematic of contact between liner and outer pipe

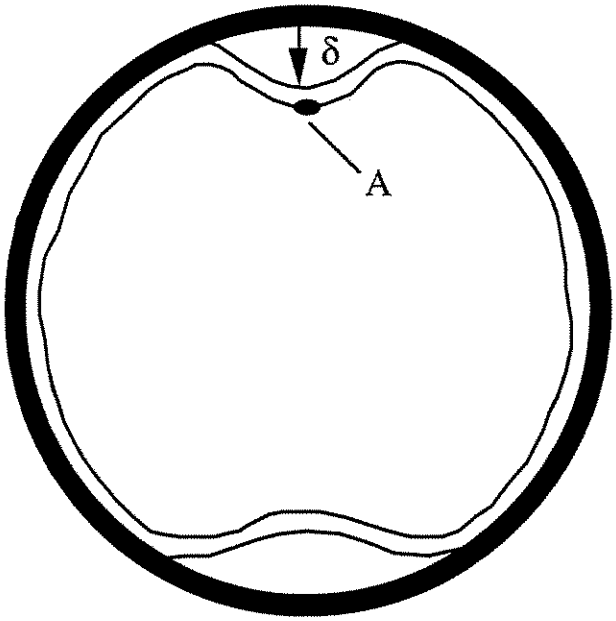

Fig. 4 - Schematic of liner deformation in a pipe

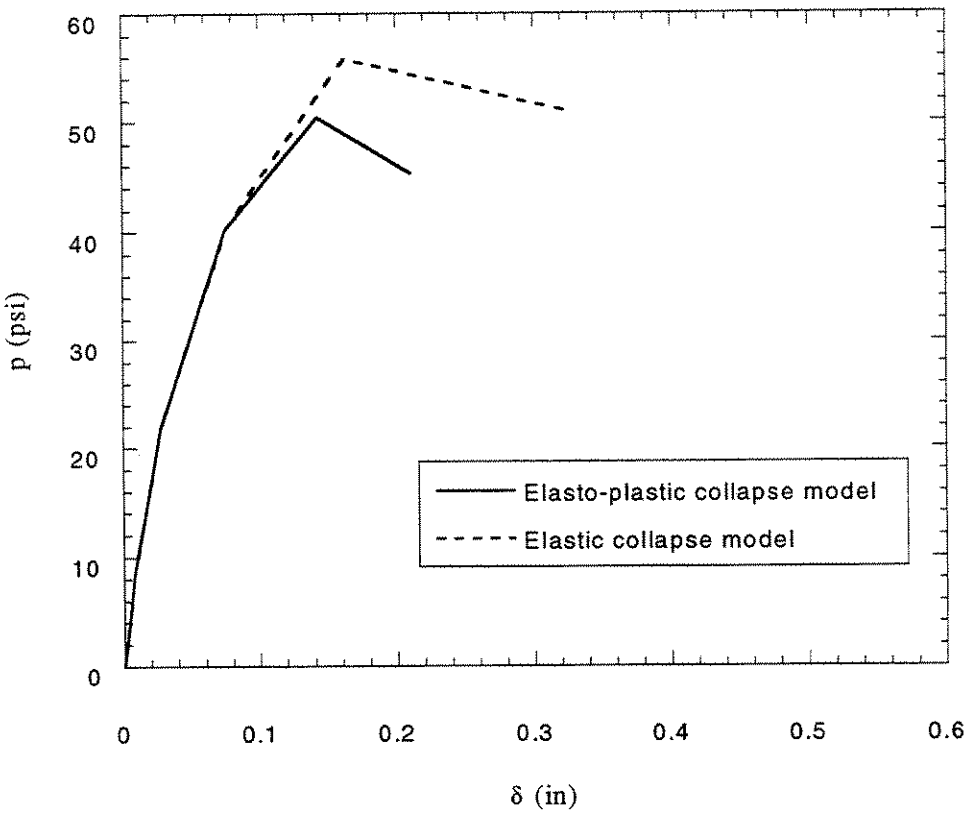

Fig. 5 - Liner separation δ and subsequent collapse of thermoplastic liner under annular pressure p (D_0 = 4.0 inch, t = 0.15 inch, η = 0).

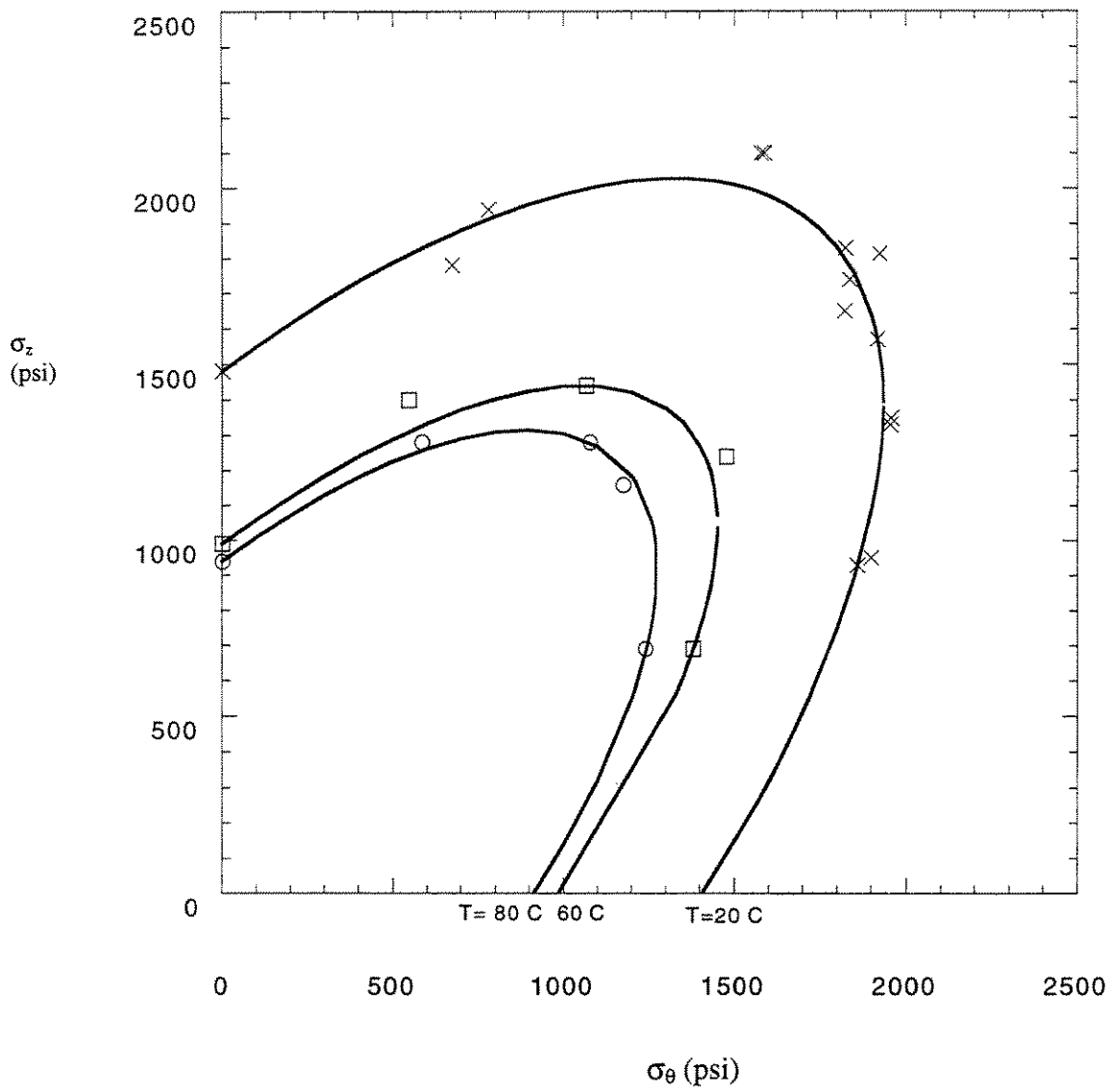

Fig. 6 – Multiaxial plastic yielding envelopes for thermoplastic liner BESNO-P40 at T=20°C, 60°C and 80°C.

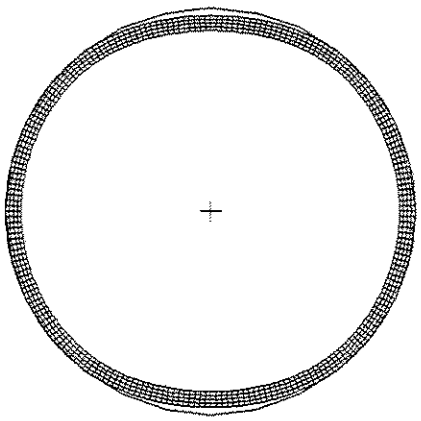

(a) p = 40.1 psi

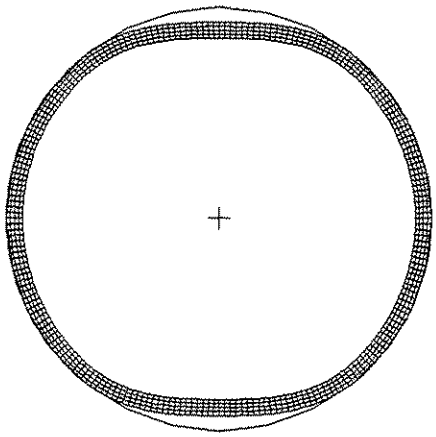

(b) p_c =50.5 psi

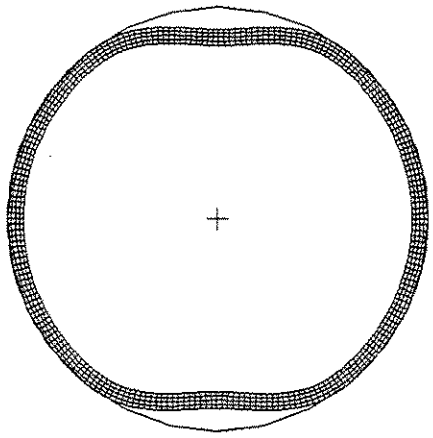

(c) p= 45.3 psi

Fig. 7 - Liner deformations at collapse and subsequent post-buckling state under annular pressure p (D_0 =4.0 inch, t =0.15 inch, η = 0).

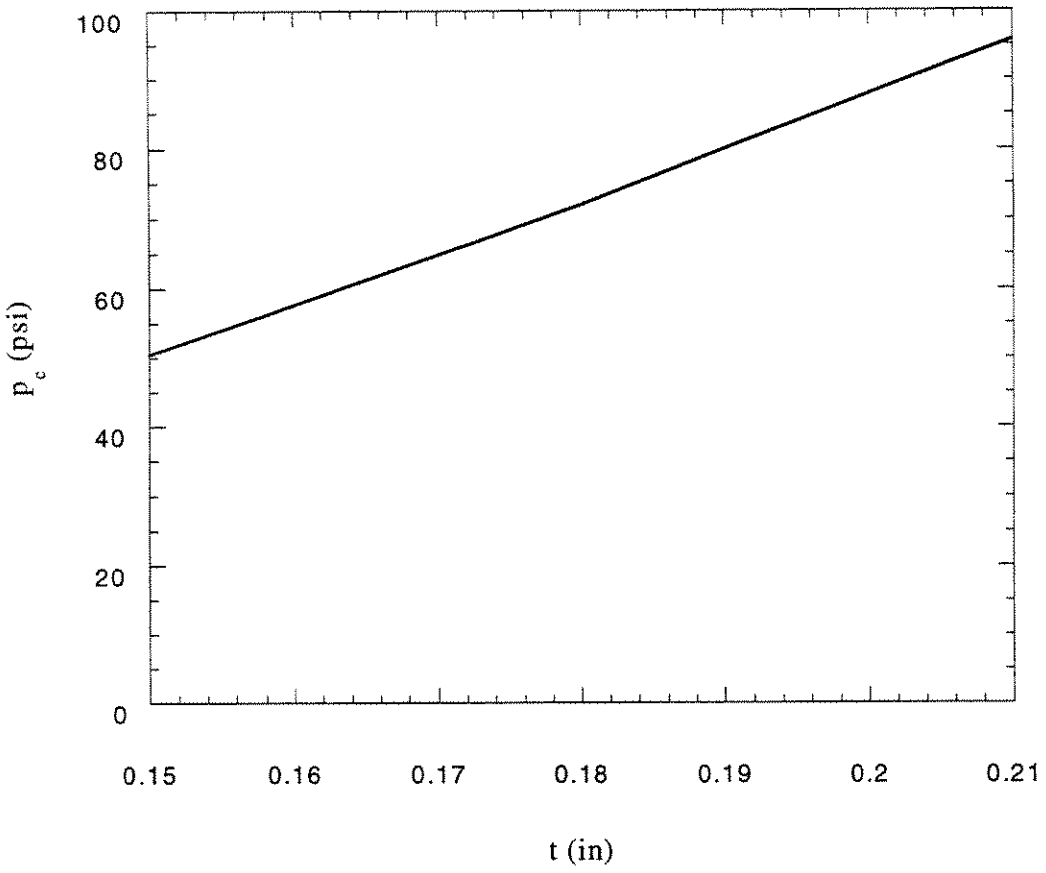

Fig. 8 - Effect of liner thickness t on critical collapse pressure p_c at room temperature ($D_0 = 4.0$ inch, $\eta = 0$).

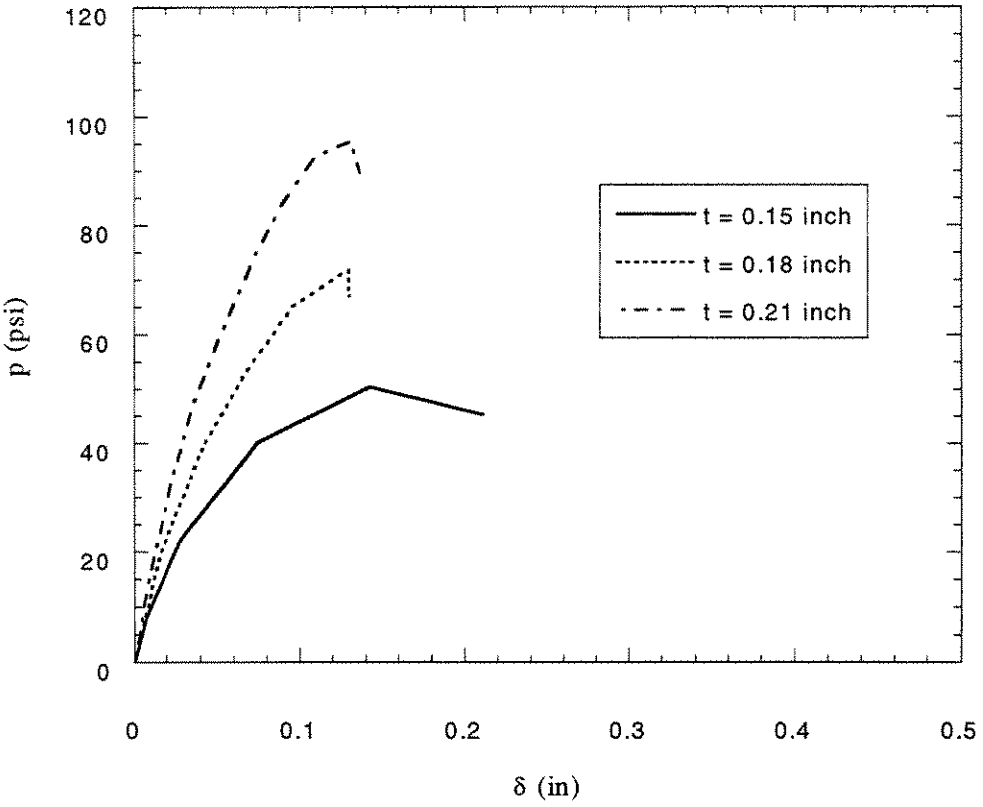

Fig. 9 - Liner separation δ and subsequent collapse with different liner thickness under annular pressure p (D_0 = 4.0 inch, η = 0).

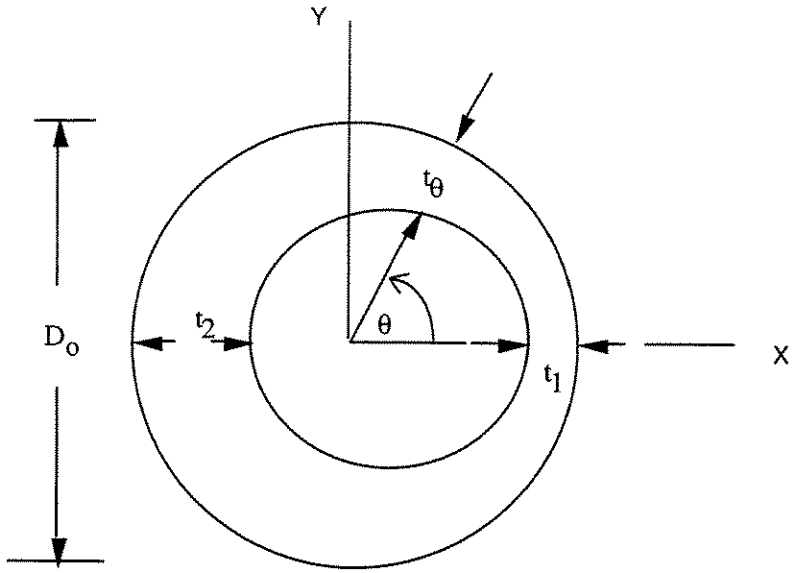

(a)

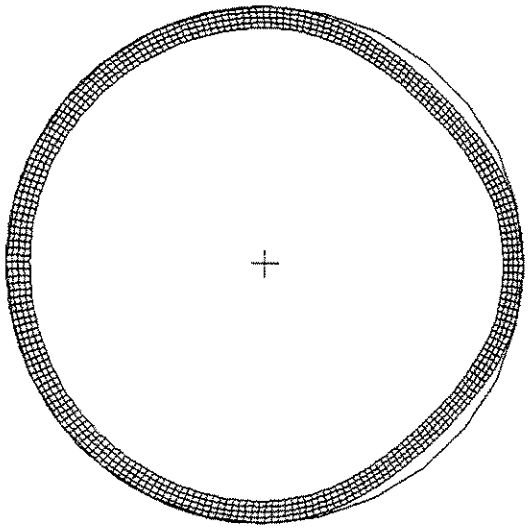

(b)

Fig.10.-(a) Liner with wall-thickness variation; (b) Liner plastic collapse mode (D_0 = 4.0 inch).

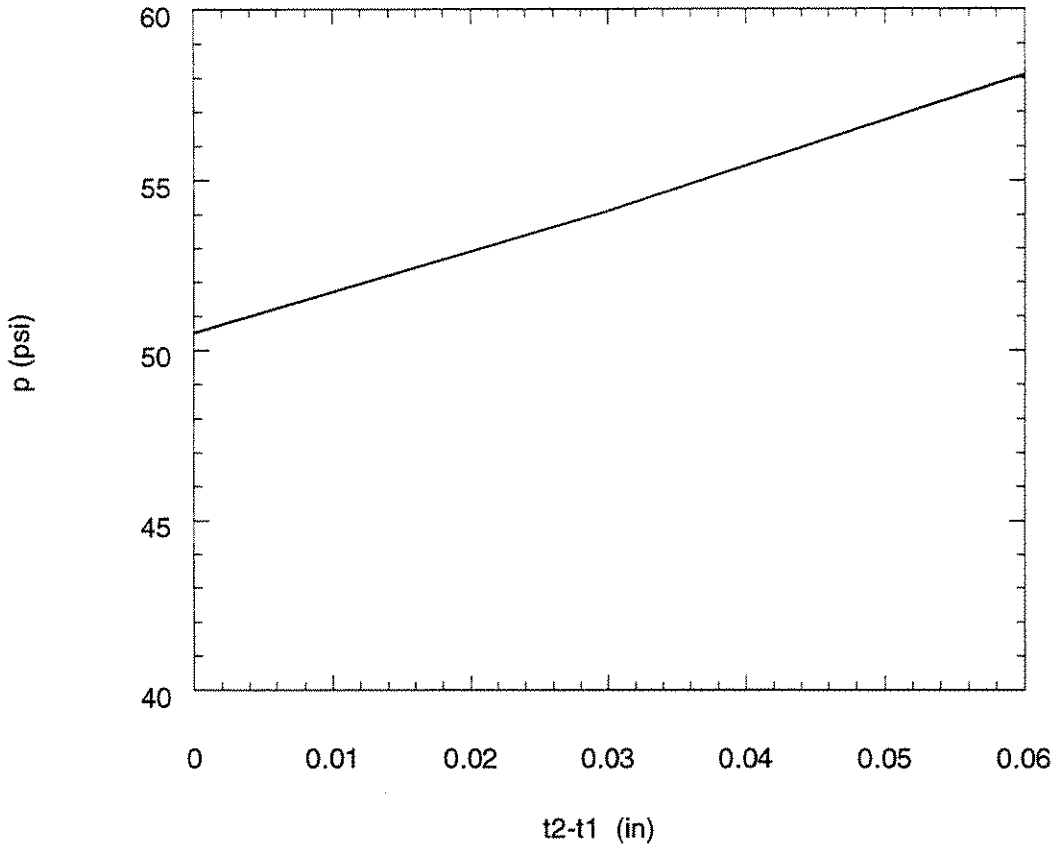

Fig. 11 - Effect of liner thickness variation (t_2-t_1) on critical collapse pressure p_c at room temperature (D_0 = 4.0 inch,η = 0).

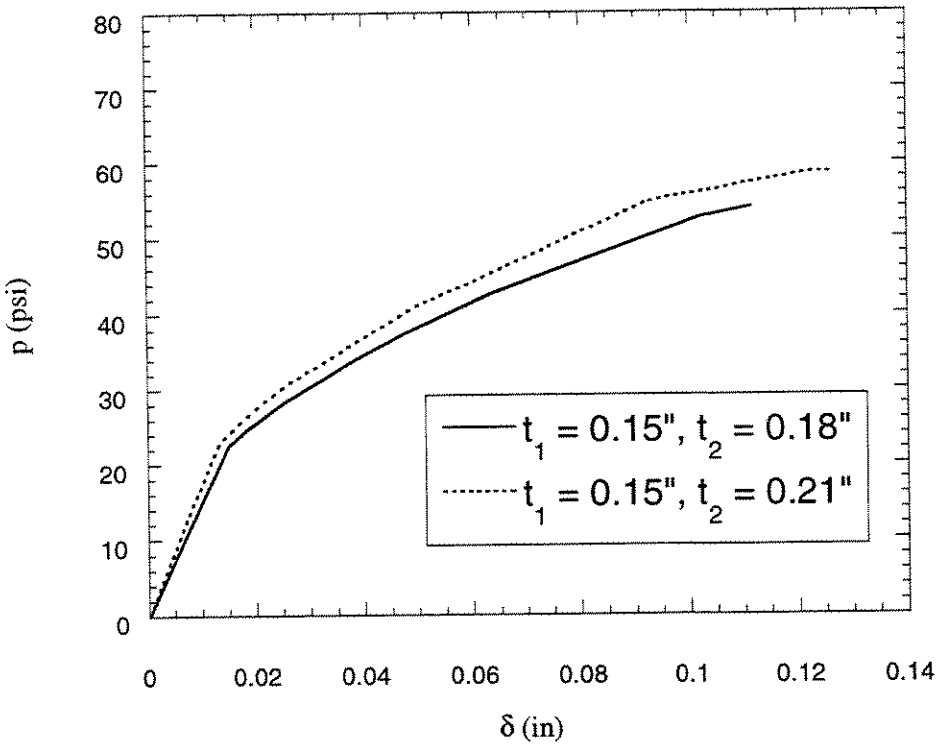

Fig. 12 - Liner separation δ and subsequent collapse with different liner wall-thickness variation under increasing annular pressure p (D_0 = 4.0 inch, η = 0).

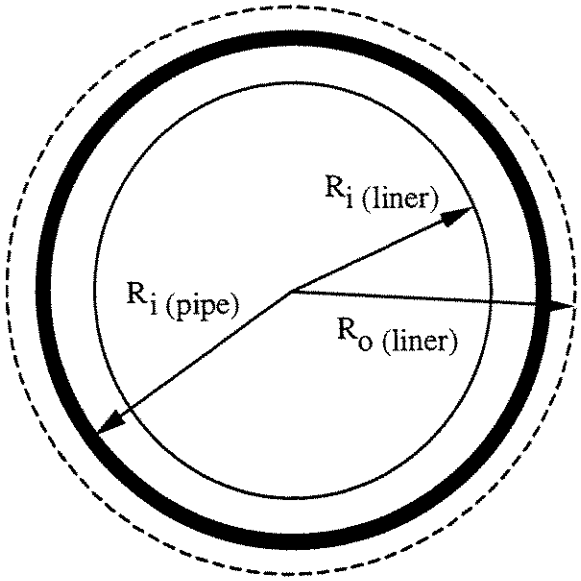

(a)Tight Fit

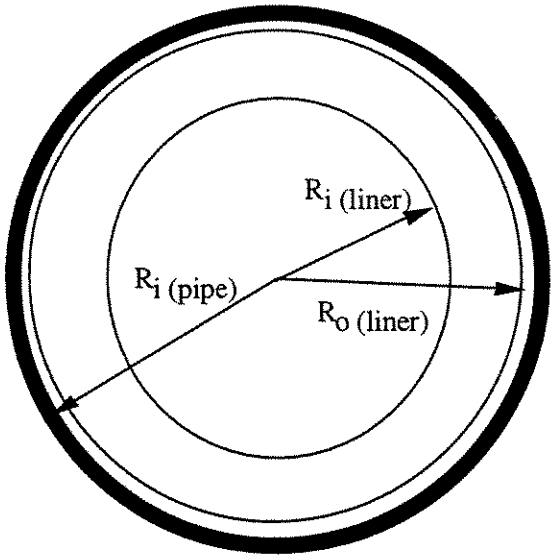

(b) loose Fit

Fig. 13 – Loose and Tight fit liners, (a) Tight fit; (b) Loose fit

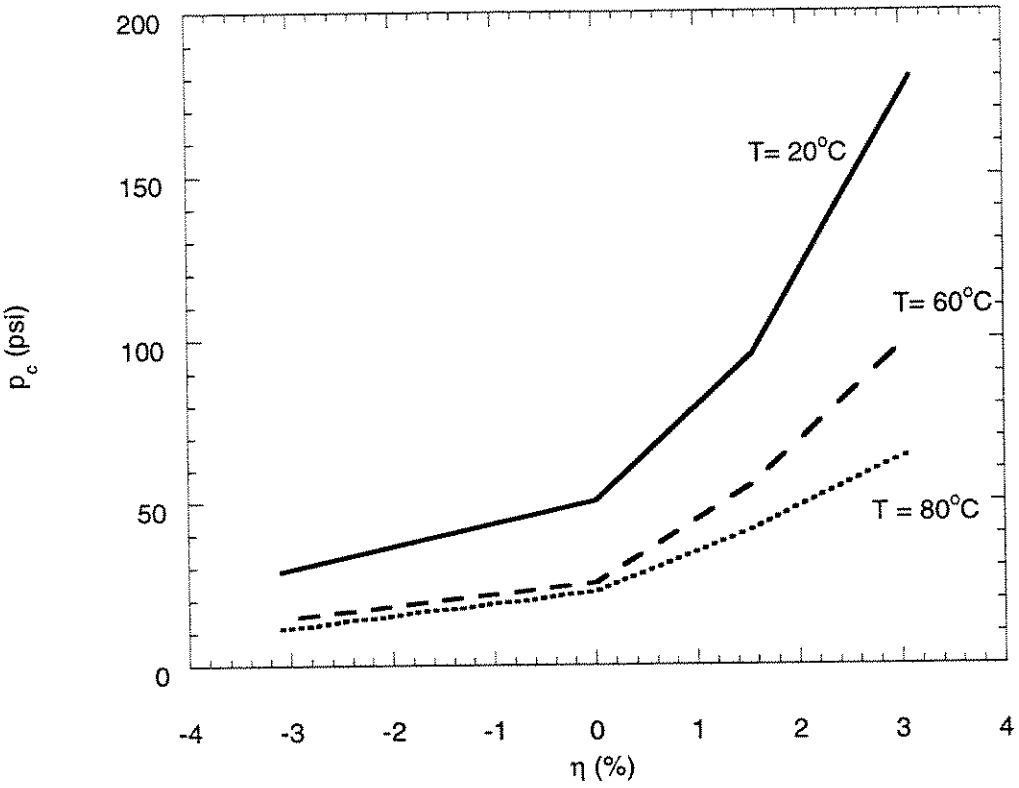

Fig. 14 - Effect of liner tightness η on critical collapse pressure p_c at different temperature (D_0 = 4.0 inch, t = 0.15 inch).

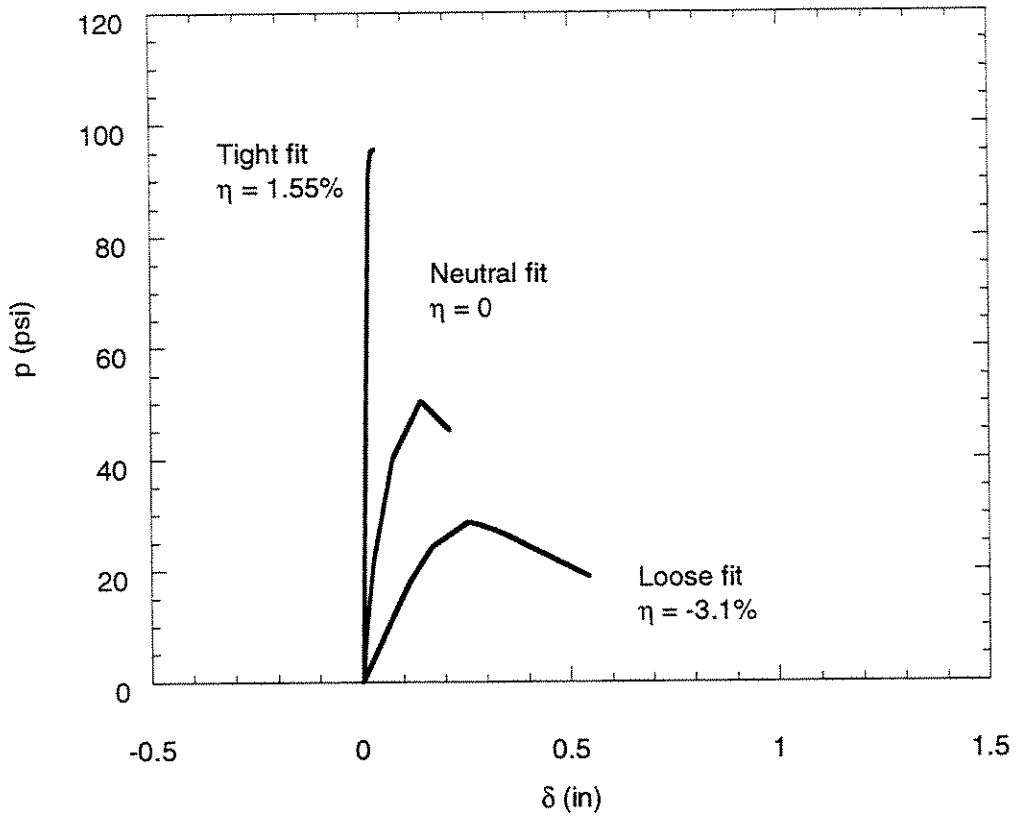

Fig. 15 - Effect of liner tightness η on liner-pipe separation δ and subsequent collapse under annular pressure p at room temperature. (D_0 = 4.0 inch, t = 0.15 inch).

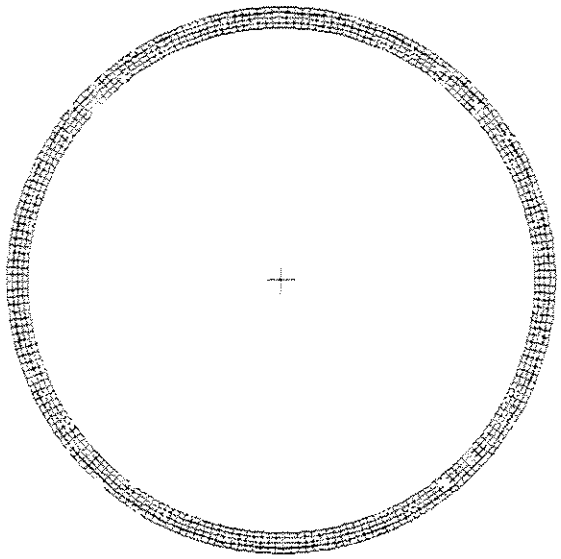

(a) Initial state

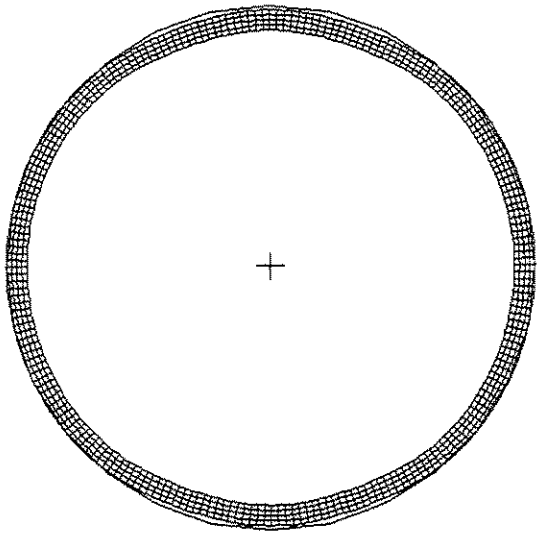

(b) at p_c = 95.6 psi

Fig. 16 - Liner deformation subjected to increasing annular pressure p (D_o = 4.0 inch, t = 0.15 inch, η = 1.55 % tightness).

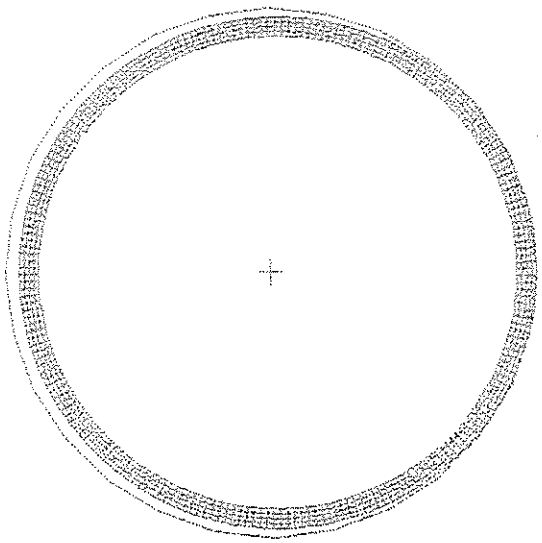

(a) Initial state

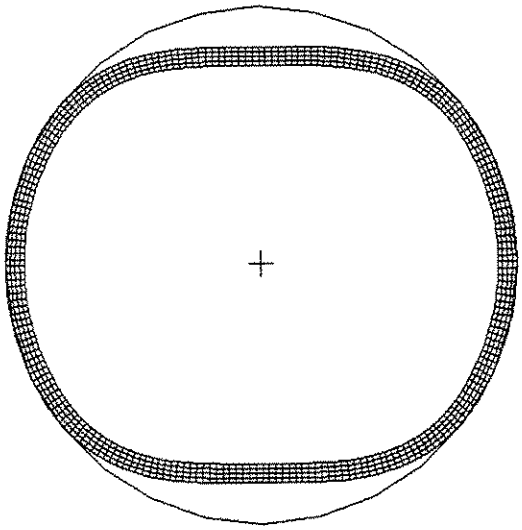

(b) at p_c = 28.8 psi

Fig. 17 - Liner deformation subjected to increasing annular pressure p (D_o = 4.0 inch, t = 0.15 inch, η = -3.1 % looseness)

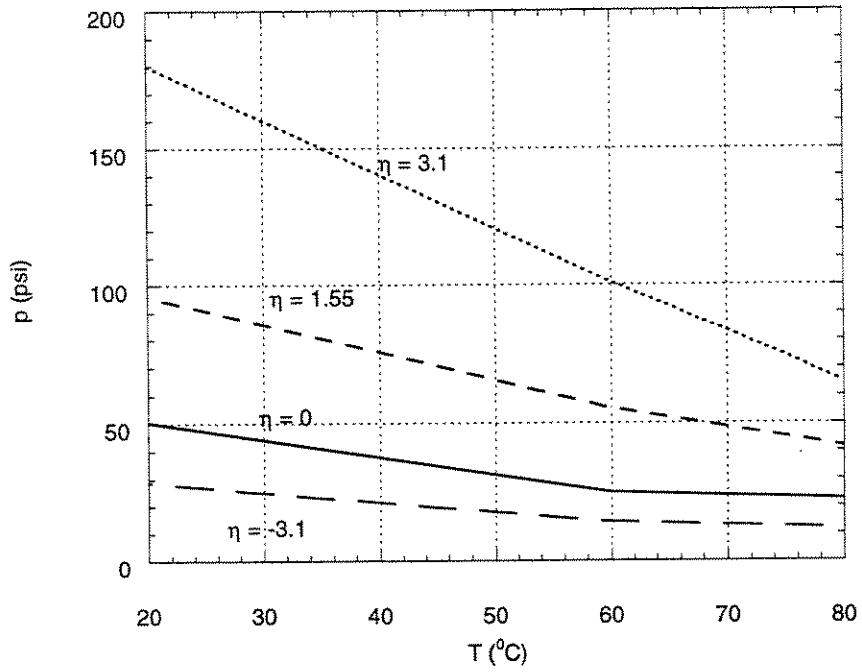

Fig. 18 - Effect of temperature on critical collapse pressure p_c of BESNO-P40 at different tightness η (D_0 =4.0 inch, t =0.15 inch).